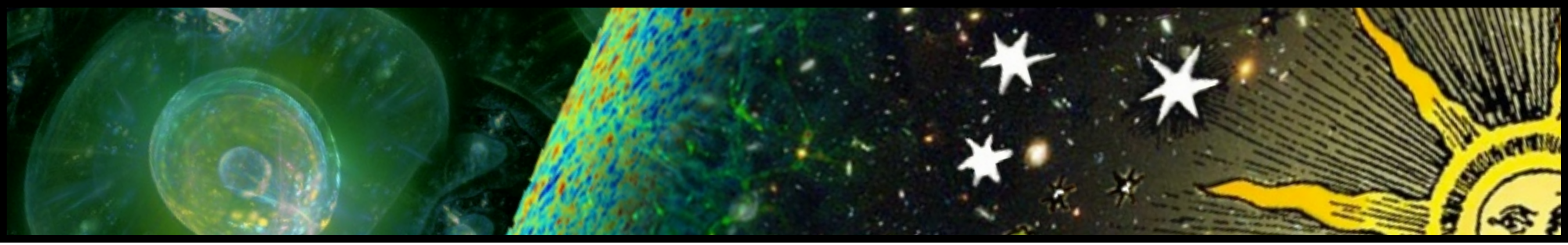

From precision to accuracy: Cosmology with large imaging surveys

Hiranya V. Peiris
University College London

Science & Technology Facilities Council

erc European Research Council

IDEAS

LSS Surveys Roadmap

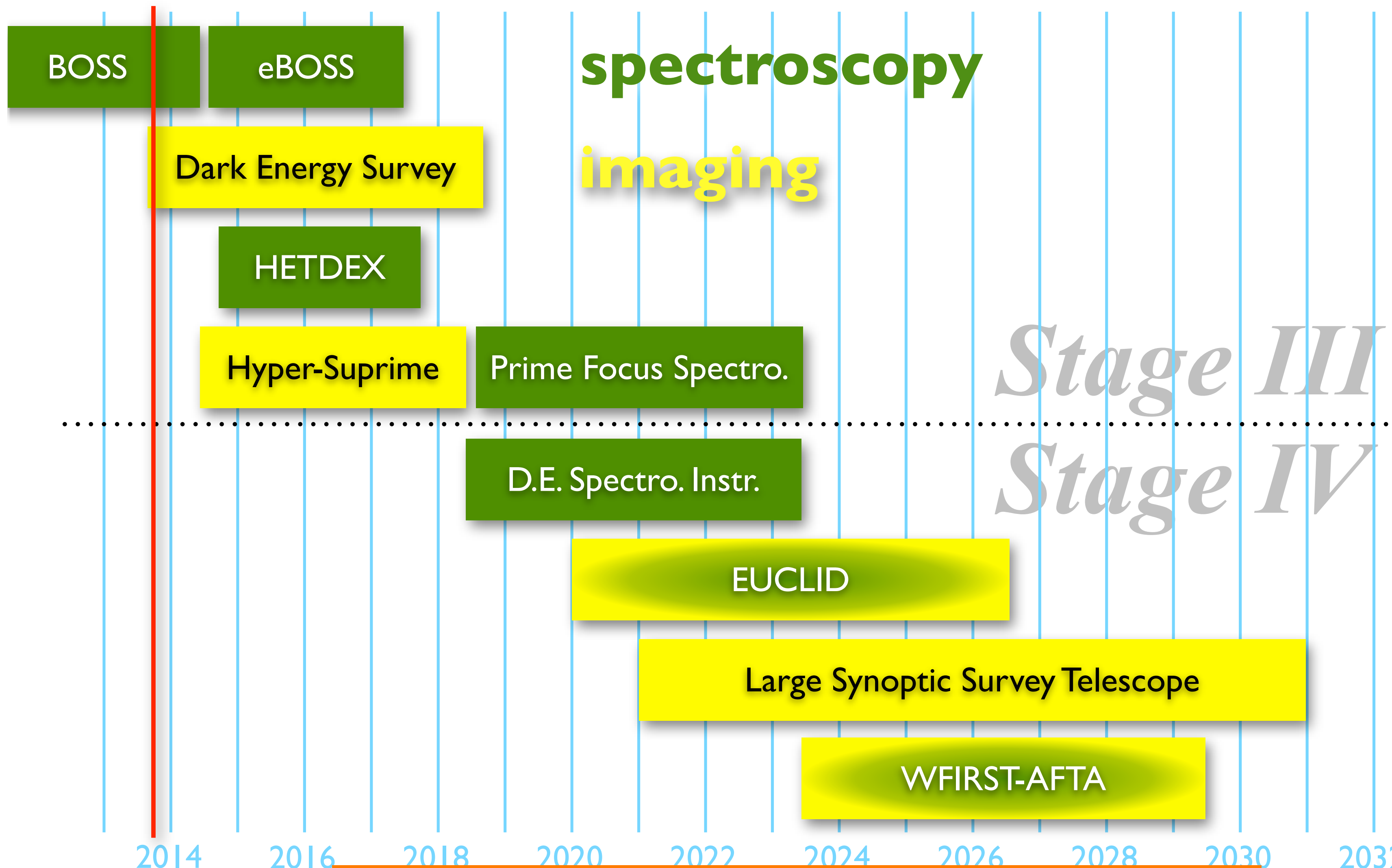

High degree of complementary between missions

Image: Ian Shipsey

“No one trusts a model except the person who wrote it; everyone trusts an observation, except the person who made it”.

H. Shapley

Known unknowns, unknown knowns, unknown unknowns

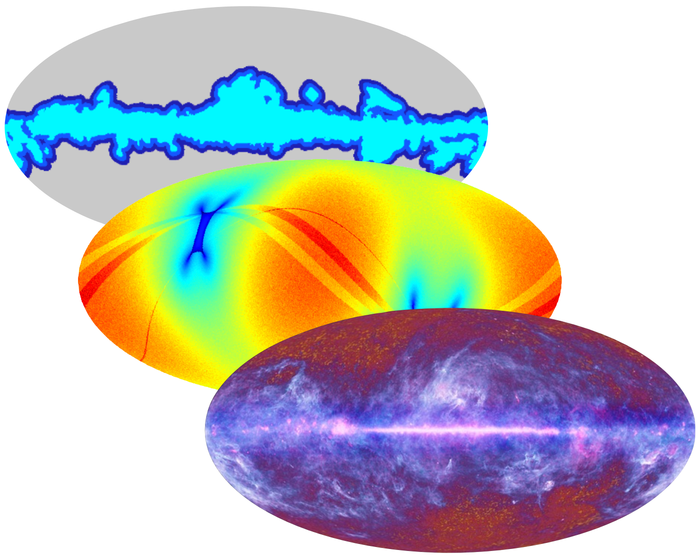

***CMB**: complex sky mask, coloured / inhomogeneous noise, foregrounds...*

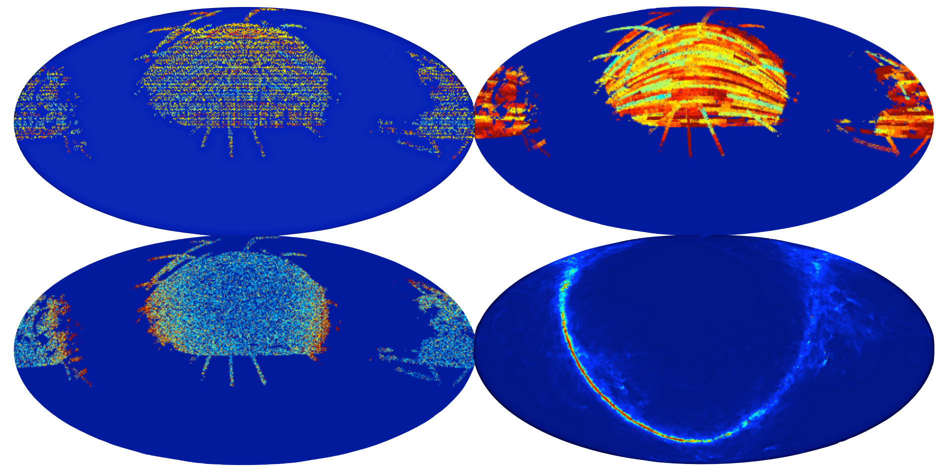

***LSS**: seeing, sky brightness, stellar contamination, dust obscuration, spatially-varying selection function, Poisson noise, photo-z errors etc...*

Need thorough understanding of data & systematics for convincing detections of new physics.

Primordial NG from the halo power spectrum

scale-dependent halo bias (Dalal et al 2008)

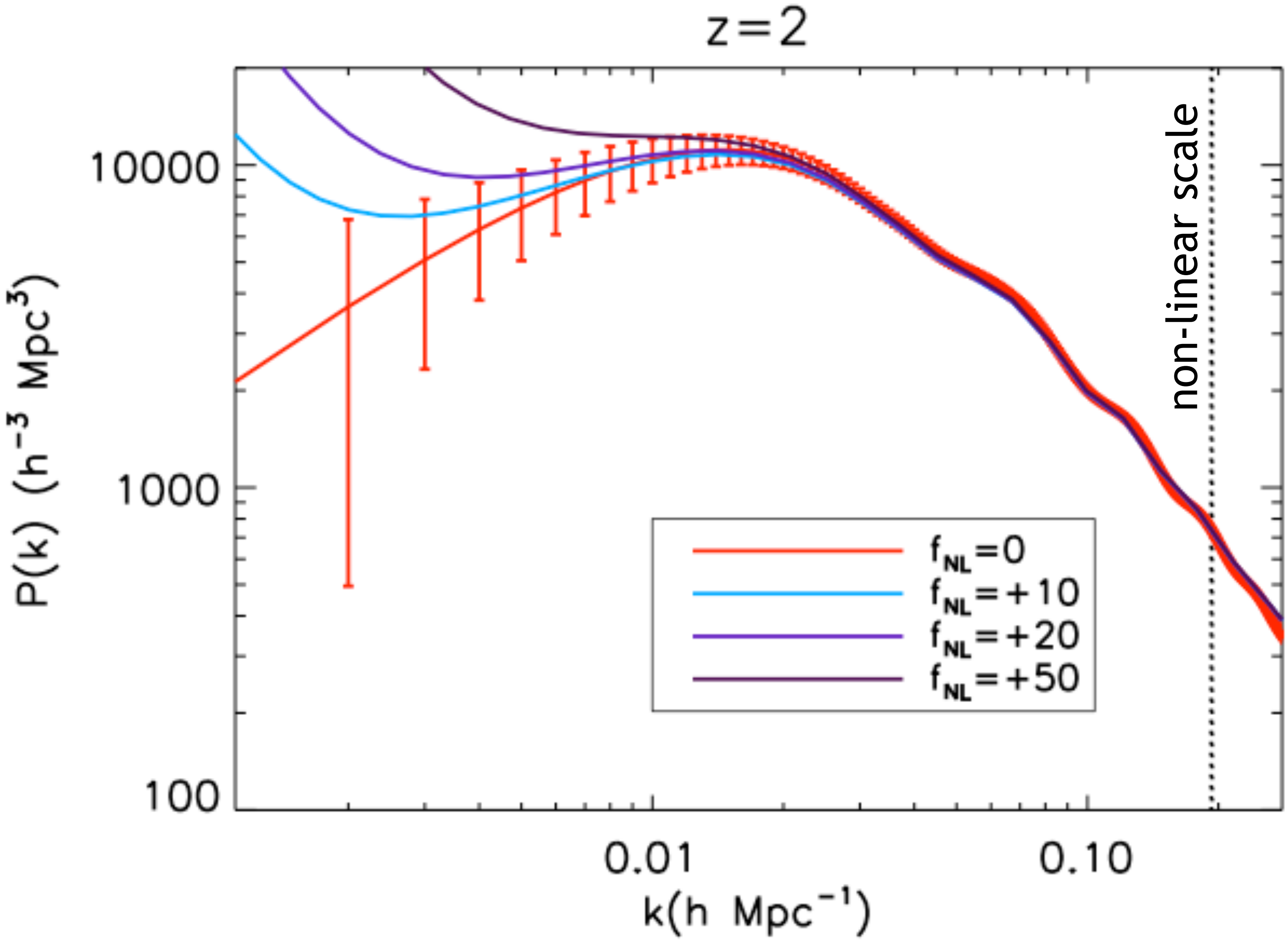

Power spectra at z=2 for a spectroscopic survey

Figure: HSLS white paper, HVP CMB/LSS Coordinator

PNG from blind mitigation of systematics in XDQSOz quasar sample

XDQSOz: 1.6 million QSO candidates from SDSS DR8 spanning z ~ 0.5-3.5 (800,000 QSOs after basic masking).

(Bovy et al.)

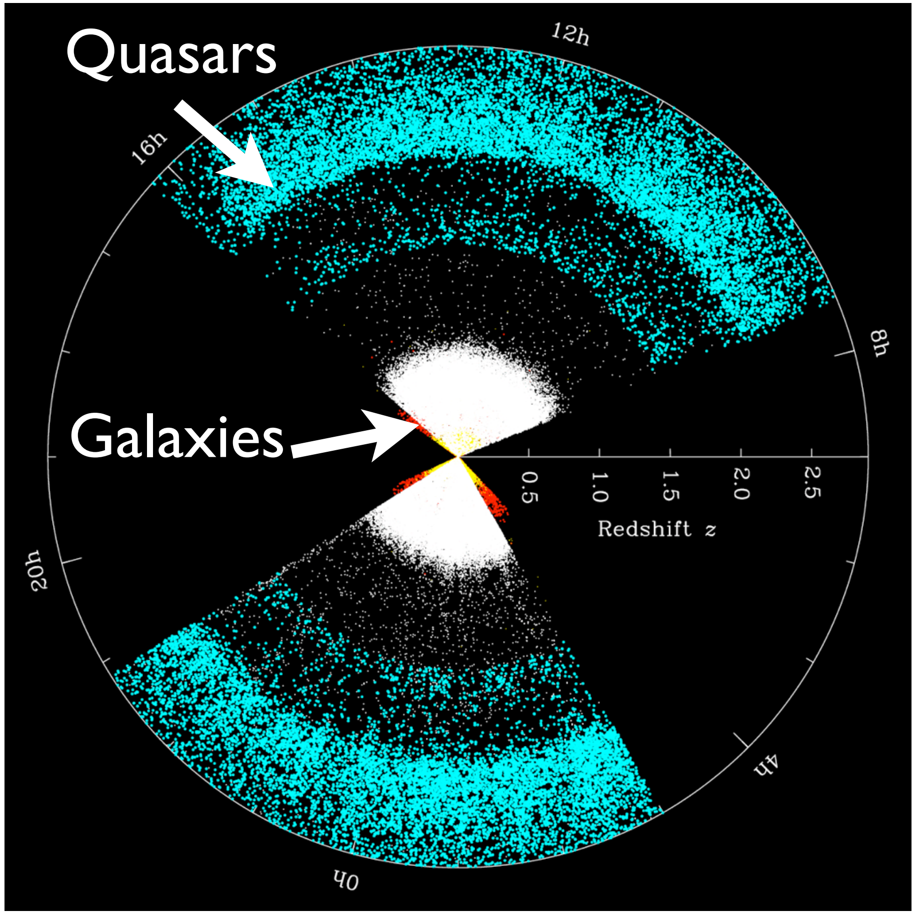

Boris Leistedt

Nina Roth

Leistedt & Peiris+ (MNRAS 2013, 2014), Leistedt, Peiris & Roth (PRL 2014)

Systematics in quasar surveys

- Anything that affects point sources or colours
  seeing, sky brightness, stellar contamination, dust obscuration, calibration etc..
- Create spatially varying depth & stellar contamination

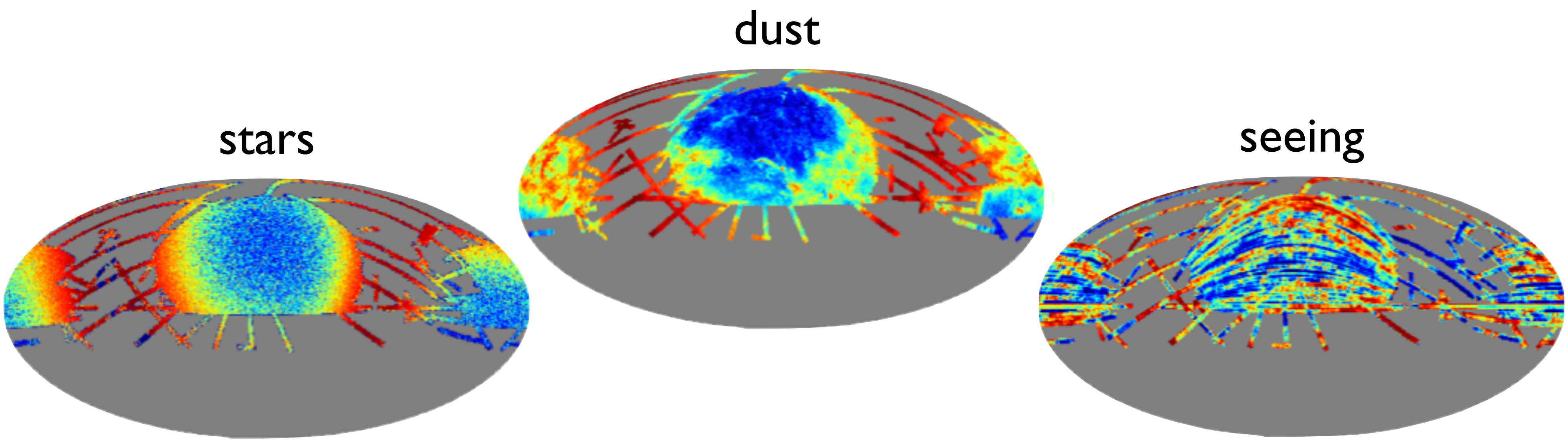

Systematics in quasar surveys

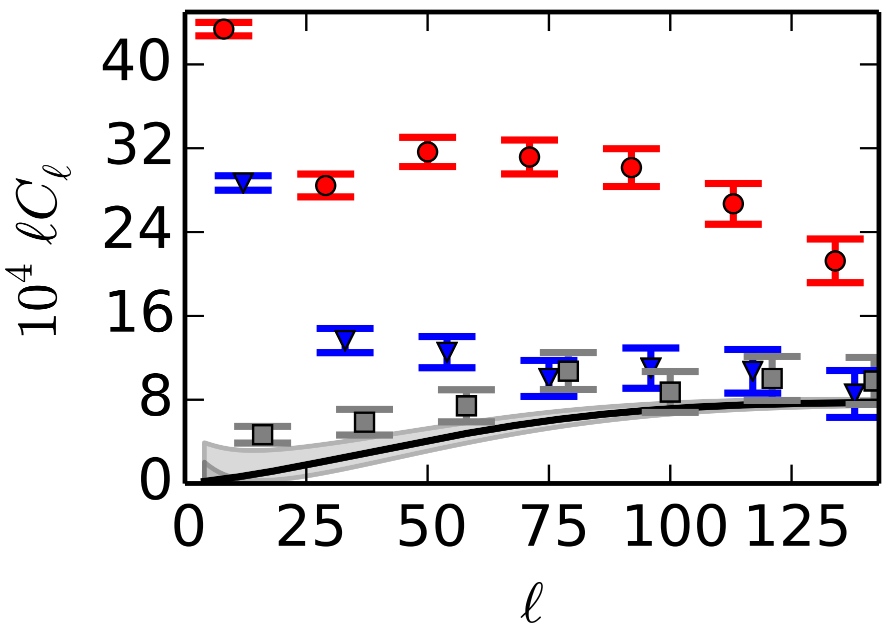

- **SDSS photometric quasars:** excess clustering power on large scales due to systematics.

- Concerns about its use for clustering studies. Pullen and Hirata 2012; Giannantonio et al. 2013

Leistedt & Peiris+ (MNRAS 2013, 1404.6530), Leistedt, Peiris & Roth (PRL 2014, 1405.4315)

Angular power spectrum estimation

- Sky masks: cuts on extinction, seeing & quality flags
- Maximum Likelihood estimator to simultaneously compute 10 auto + cross angular power spectra

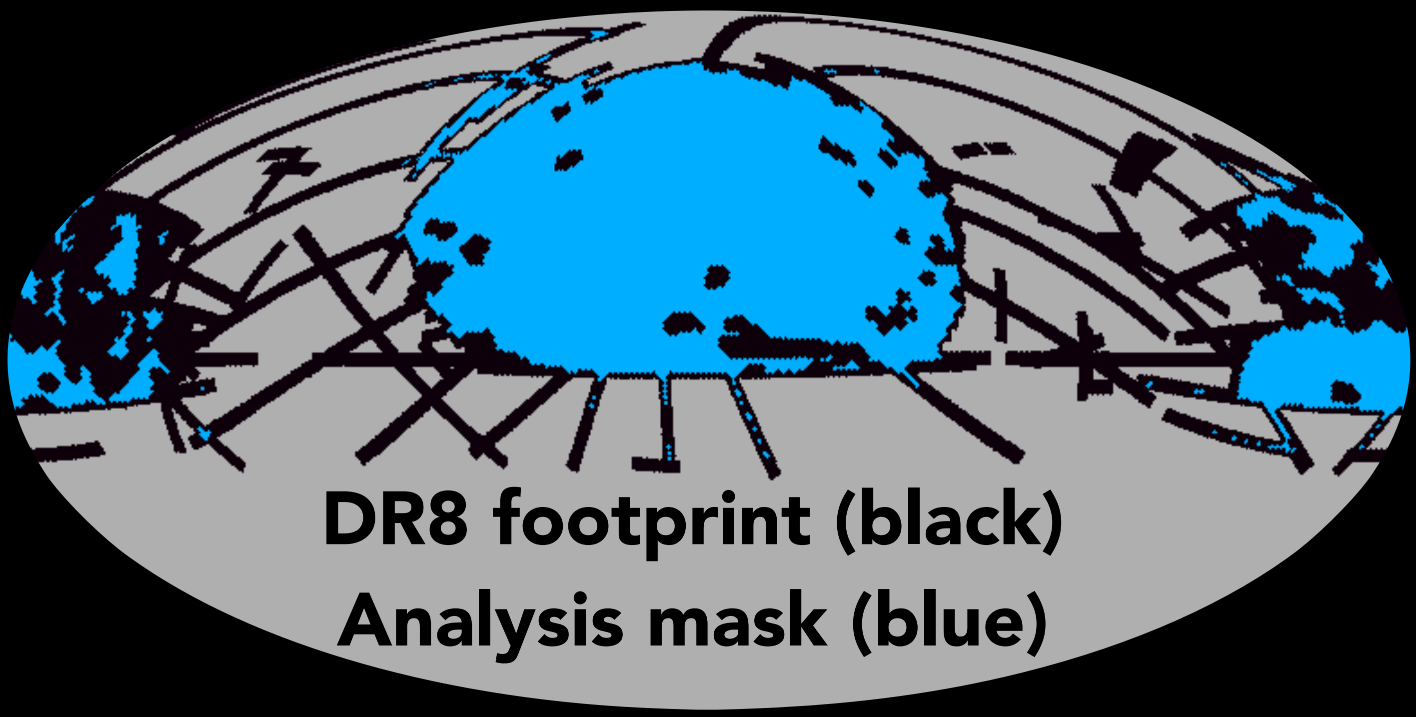

Systematics and mode projection

Rybicki and Press (1992)

- PCL suboptimal with complex masks and systematics
- QML with mode projection: marginalises over linear contamination models, using systematics templates $\vec{c}_k$

$$\mathbf{C} \;=\; \sum_{\ell} \mathcal{C}_\ell \mathbf{P}_\ell + \mathbf{N} + \sum_{k \in \mathrm{sys}} \xi_k \vec{c}_k \vec{c}_k^{\,t} \quad \text{with} \;\; \xi_k \to \infty$$

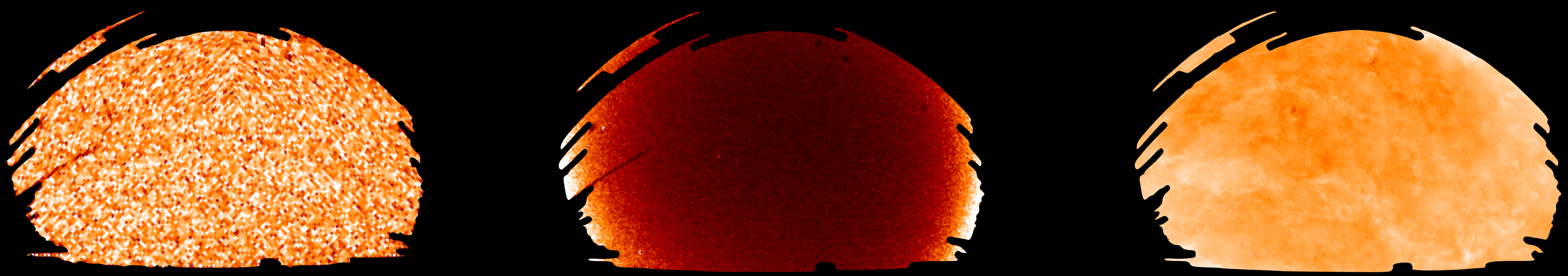

quasar catalogue — stars — dust extinction

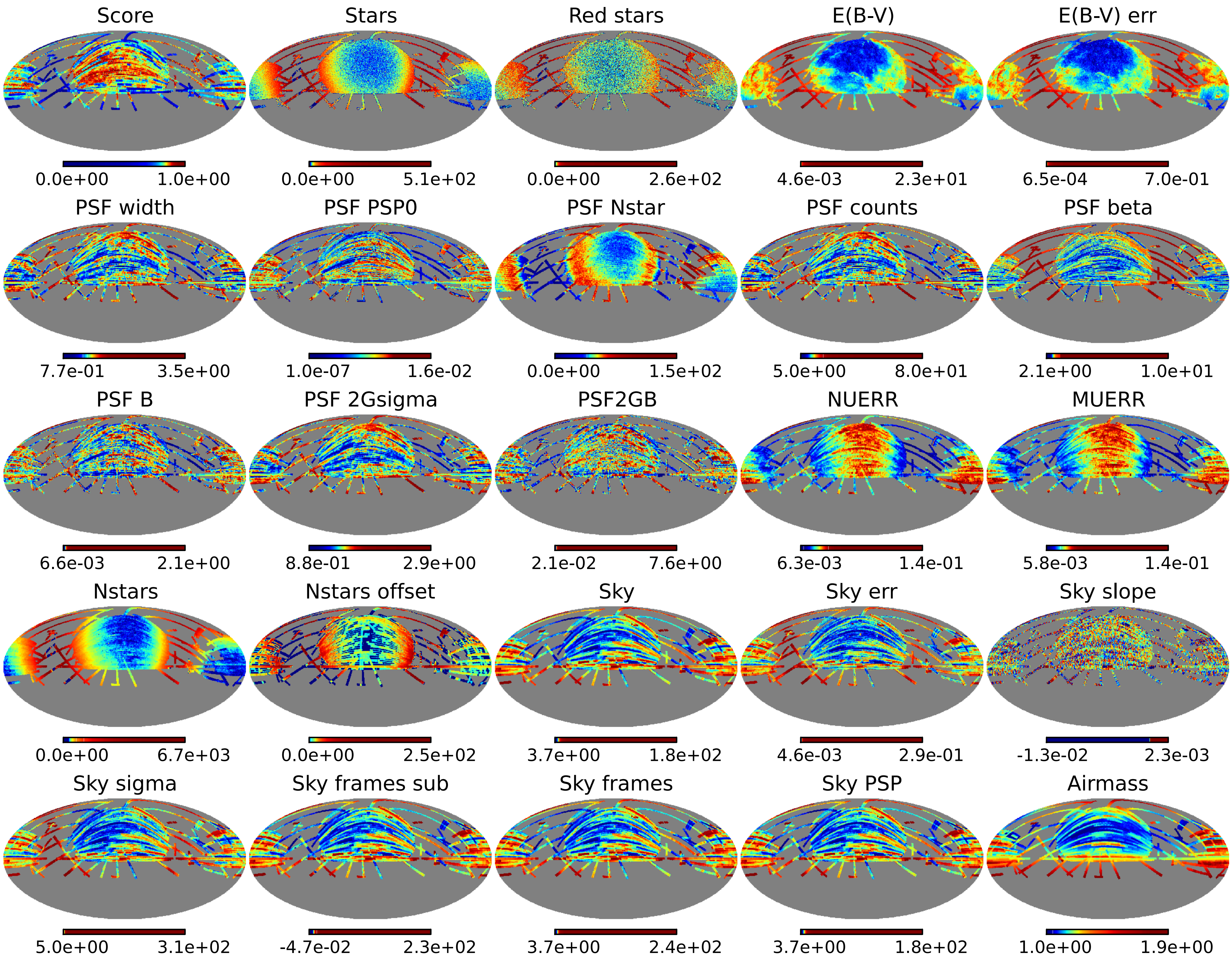
Score
0.0e+00
1.0e+00
Stars
0.0e+00
5.1e+02
Red stars
0.0e+00
2.6e+02
E(B-V)
4.6e-03
2.3e+01
E(B-V) err
6.5e-04
7.0e-01
PSF width
7.7e-01
3.5e+00
PSF PSP0
1.0e-07
1.6e-02
PSF Nstar
0.0e+00
1.5e+02
PSF counts
5.0e+00
8.0e+01
PSF beta
2.1e+00
1.0e+01
PSF B
6.6e-03
2.1e+00
PSF 2Gsigma
8.8e-01
2.9e+00
PSF2GB
2.1e-02
7.6e+00
NUERR
6.3e-03
1.4e-01
MUERR
5.8e-03
1.4e-01
Nstars
0.0e+00
6.7e+03
Nstars offset
0.0e+00
2.5e+02
Sky
3.7e+00
1.8e+02
Sky err
4.6e-03
2.9e-01
Sky slope
-1.3e-02
2.3e-03
Sky sigma
5.0e+00
3.1e+02
Sky frames sub
-4.7e-02
2.3e+02
Sky frames
3.7e+00
2.4e+02
Sky PSP
3.7e+00
1.8e+02
Airmass
1.0e+00
1.9e+00

Extended mode projection

- Create set of input systematics

  220 templates + pairs ⇒ >20,000 templates

- Decorrelate systematics

  20,000 templates ⇒ 3,700 uncorrelated modes

- Ignore modes most correlated with data

  3,700 null tests; project out modes with red chi2>1

Sacrificing some signal in favour of robustness
⇒ **Blind mitigation of systematics**

Leistedt & Peiris+ (MNRAS 2013, 1404.6530), Leistedt, Peiris & Roth (PRL 2014, 1405.4315)

Extended mode projection

- **Masking in a rotated basis:** *rather than correcting data, project out potentially contaminated modes (estimator variance self-consistently inflated).*

- **Data-driven contamination model:** *don't choose by hand which systematics to concentrate on.*

- **Blind mitigation:** *pre-fixed criterion for systematics residuals threshold.*

Leistedt & Peiris+ (MNRAS 2013, 1404.6530), Leistedt, Peiris & Roth (PRL 2014, 1405.4315)

Blind mitigation of systematics

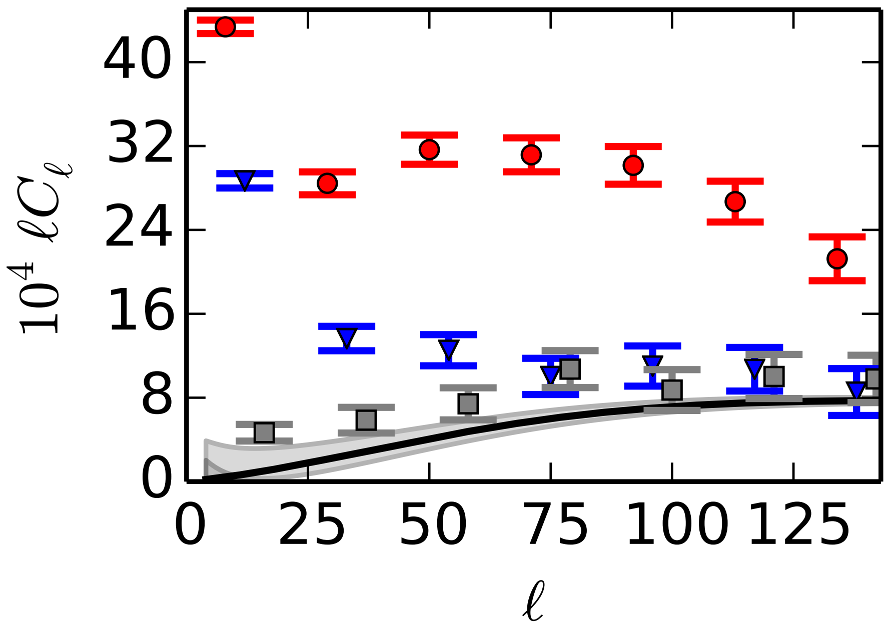

Raw spectra

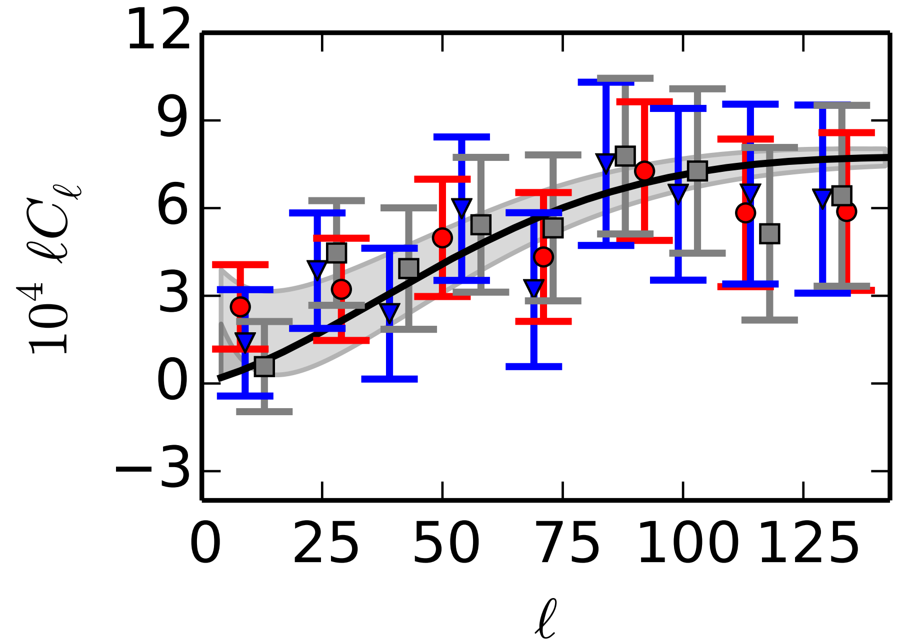

Clean spectra

- Example: one of 10 spectra (auto + cross in four z-bins) in likelihood

- Grey bands: -50 < f_{NL} < 50; colours: basic masking + m.p.

Leistedt & Peiris+ (MNRAS 2013, 1404.6530), Leistedt, Peiris & Roth (PRL 2014, 1405.4315)

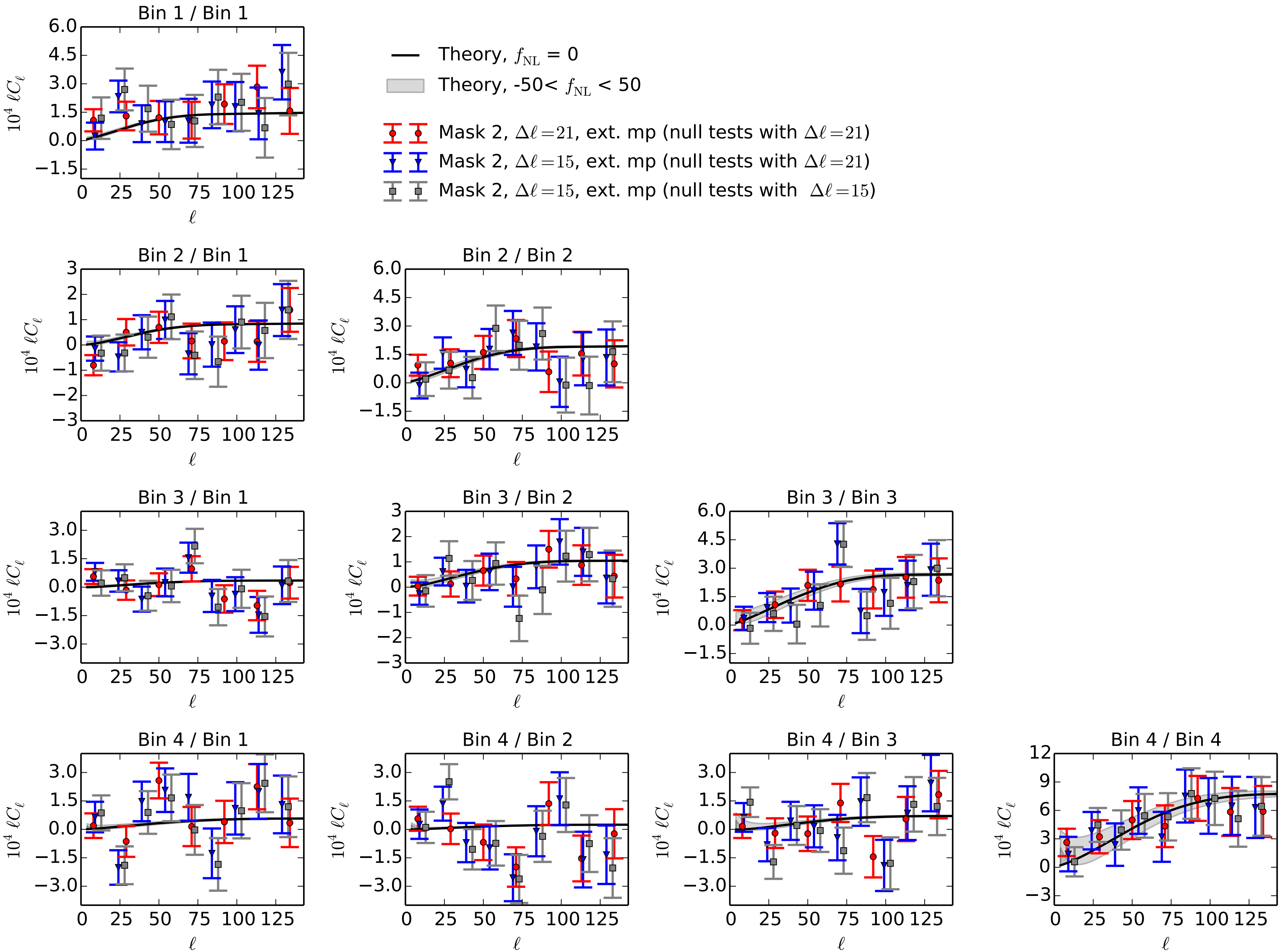

Leistedt & Peiris+ (MNRAS 2013, 1404.6530), Leistedt, Peiris & Roth (PRL 2014, 1405.4315)

Theory

Ingredients for computing theory power spectra:

- Cosmological parameters (LCDM + $f_{\rm NL}$)
- Redshift distribution, shot noise, nb count slope
- Quasar bias model: $b(z) = b_0 \left[1 + \left(\frac{1+z}{\alpha} \right)^{\beta} \right]$

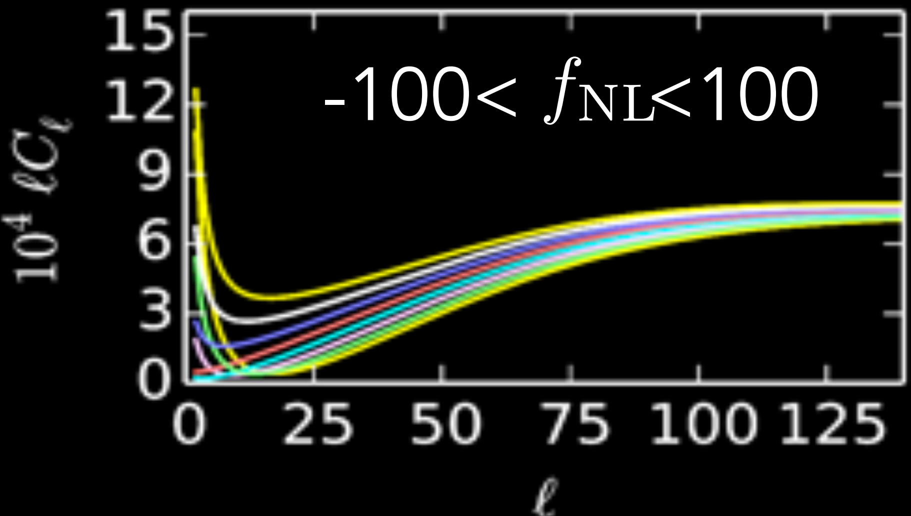

PNG: enhances large scale quasar bias

Used **emcee** (Foreman-Mackey et at 2013) + **CAMB_sources** (Challinor & Lewis 2011)

Photometric redshift estimates

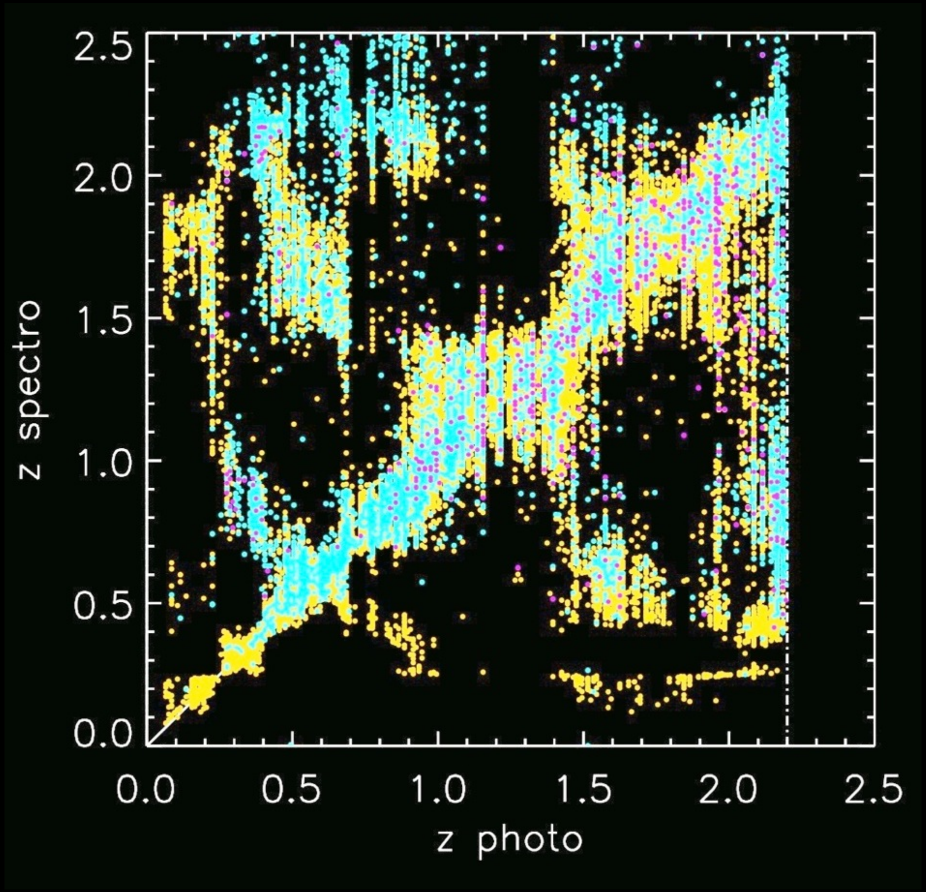

Cross-matching RQCat with SDSS-DR7, BOSS, and 2SLAQ

- Quasar photo-z have large fraction of outliers
- Redshift distributions poorly known
- Impacts robustness of theory power spectra

Analysis of XDQSOz quasars

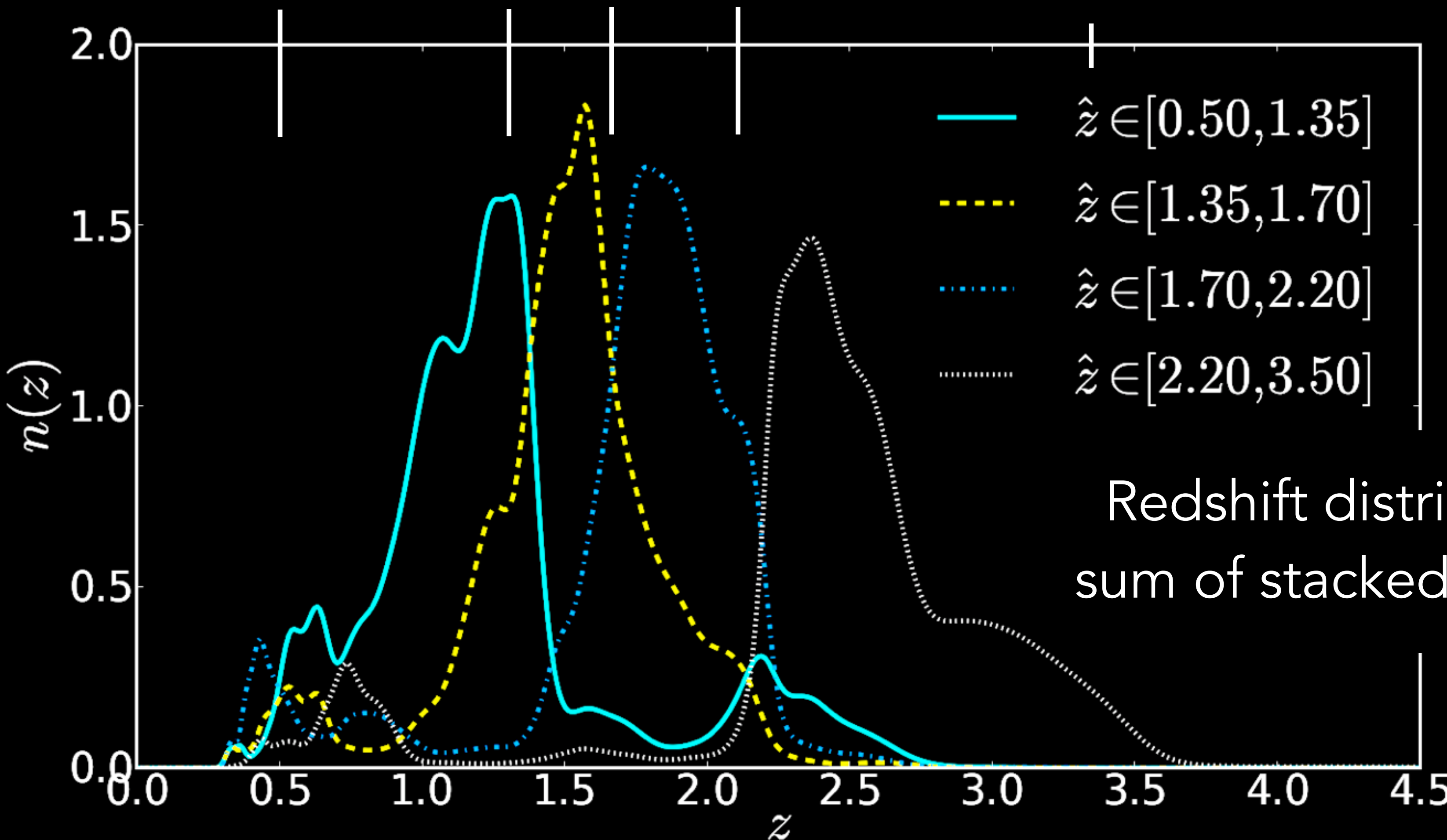

Redshift distributions = sum of stacked posteriors

arXiv: 1404:6530

Constraints on f_{NL}

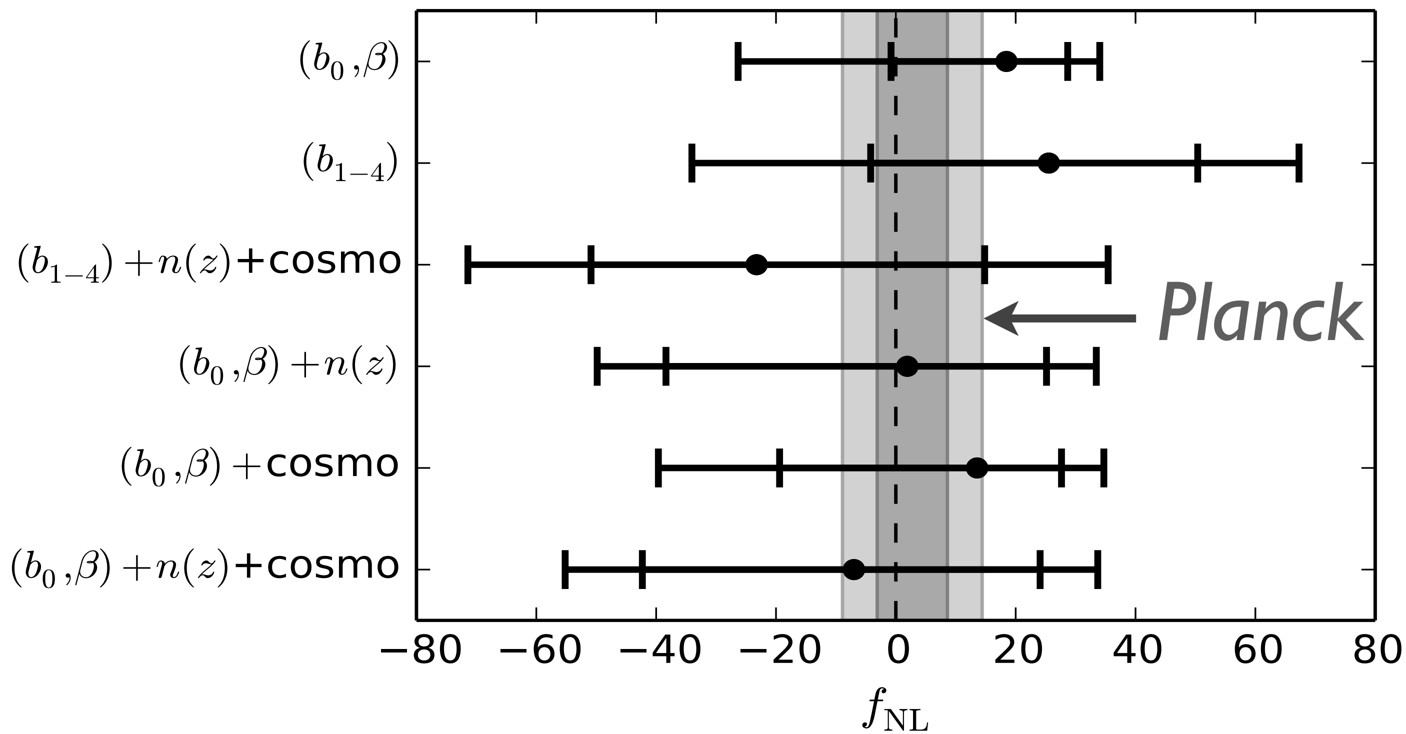

$-16 < f_{\rm NL} < 47 \ (2\sigma)$ — *Fixed cosmology & n(z)*

$-49 < f_{\rm NL} < 31 \ (2\sigma)$ — *Varying all parameters*

- Comparable to WMAP9 from single LSS tracer(!)
- Robust to modelling & priors

Leistedt, Peiris & Roth (PRL 2014, 1405.4315)

LSST survey of 18,000 sq deg

(half the sky)

Large Synoptic Survey Telescope

- **LSST forecast:**
  - expected statistical $\sigma(f_{NL}) < 1$
  - systematic bias for a contamination model f_{NL} ~30,
  - correcting bias leads to conservative forecast $\sigma(f_{NL})$~ 5.

Leistedt, Peiris & Roth (PRL 2014, 1405.4315)

The Dark Energy Survey (DES)

300 million galaxies over 1/8 of the sky

DARK ENERGY
SURVEY

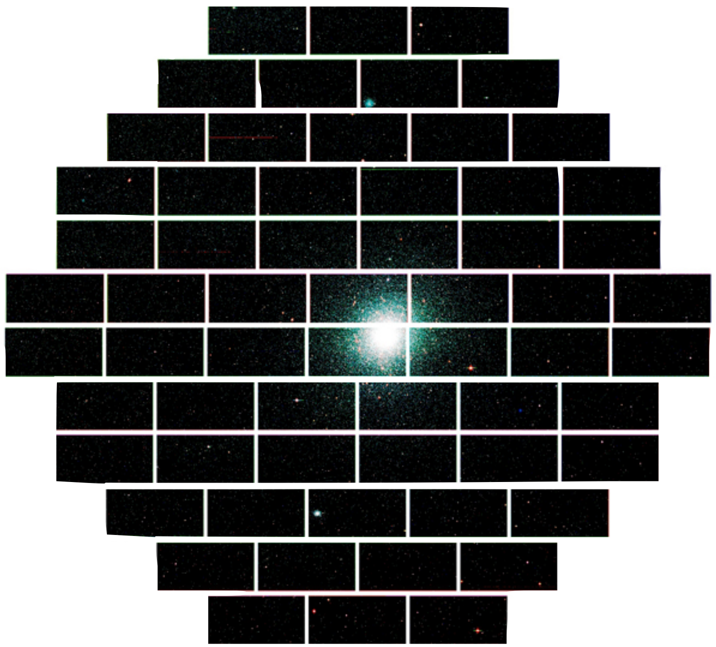

- 4-m Blanco
- 570 Mpix camera (DECam)
- 2.2 deg field of view
- Cerro Tololo (CTIO), Chile
- second year of 5-yr survey

Mapping spatially-varying properties of DES

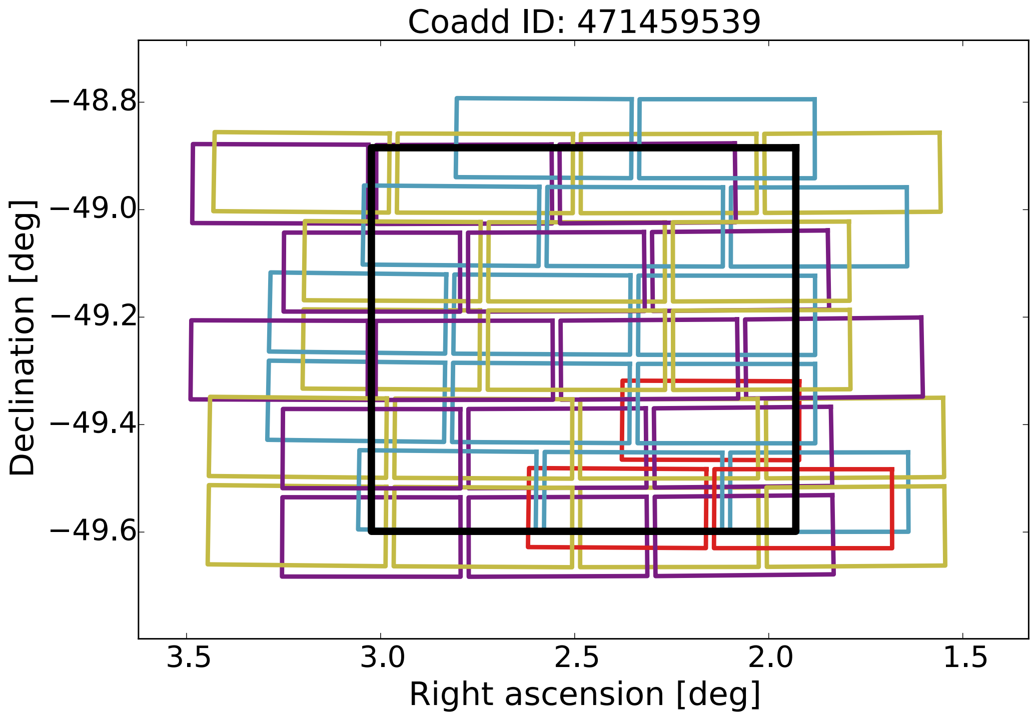

- **Geometrical projection** of single-exposure images coadded in arbitrary tile (black) of DES Science Verification data.
- **Colours:** different pointings, each with 62 single-epoch images corresponding to camera CCDs.

Leistedt, Peiris, Elsner et al. (DES Collaboration), 2015 in prep

Mapping spatially-varying properties of DES

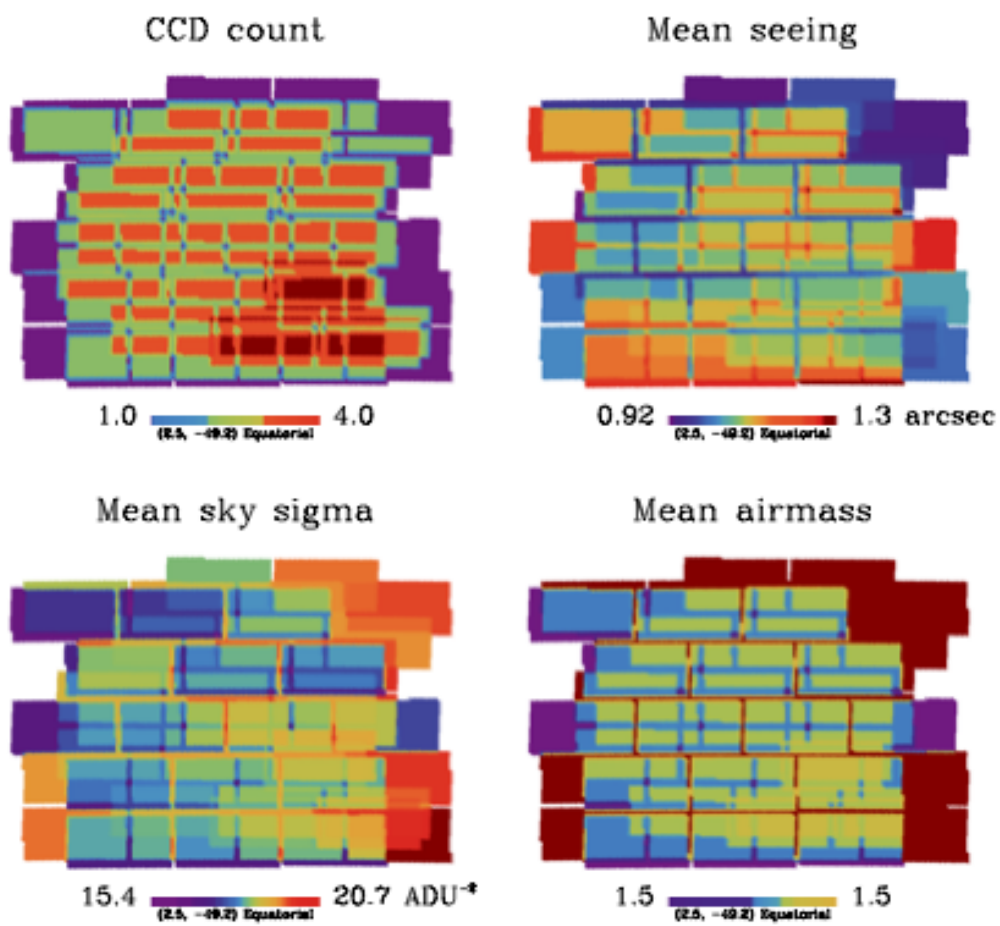

- **Projection** of single-epoch image properties: time fluctuations & correlations are converted into spatial fluctuations.

Leistedt, Peiris, Elsner et al. (DES Collaboration), 2015

Spatially-varying systematics on SV footprint

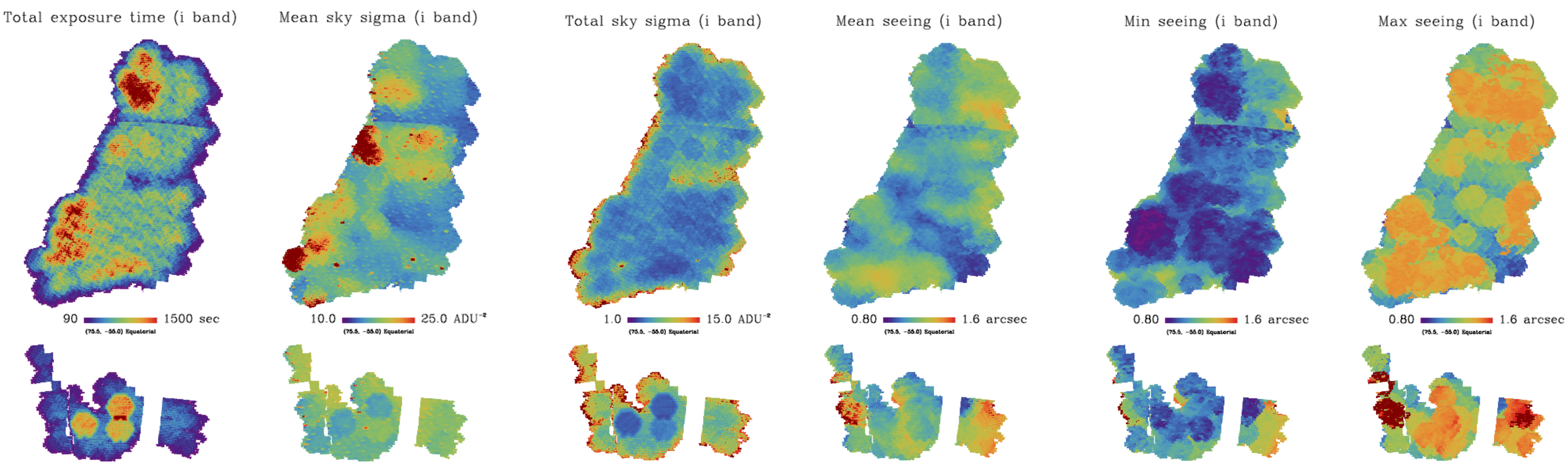

- Leistedt et al projection algorithm is now data product incorporated into DES pipeline.
- Used to investigate impact on clustering studies (LSS/shear/lensing), photo-z estimation, star/galaxy separation, survey depth fluctuations….

Leistedt, Peiris, Elsner et al. (DES Collaboration), 2015

Incorporated in end-to-end image simulations

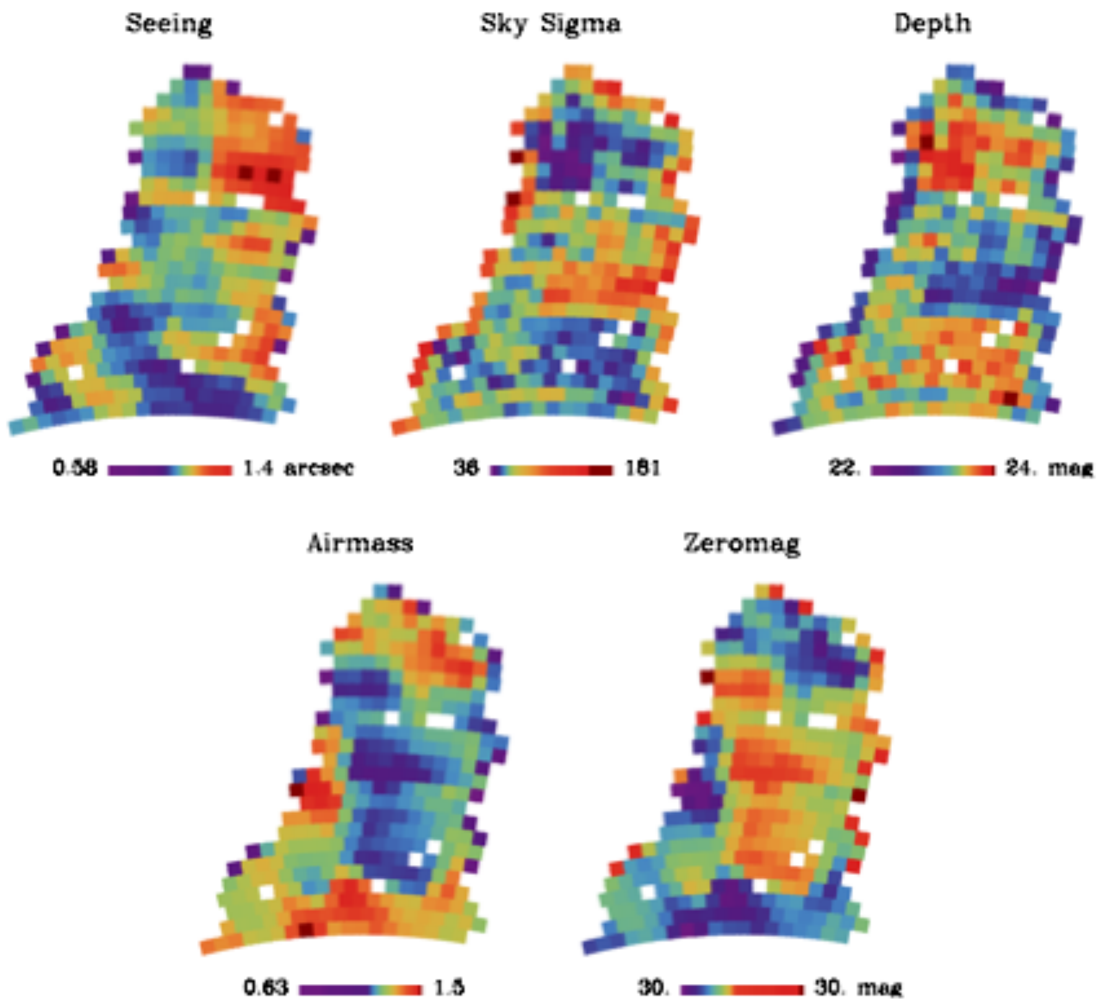

- **BCC-UFig:** Forward image simulations of SV data (based on Blind Cosmology Challenge simulations and Ultra-Fast Image Generator)

Busha et al (2013), Bergé et al (2013) Chang et al. (DES Collaboration, 2014)

Conclusions and Outlook

- **XDQSOz:** expected statistical $\sigma(f_{NL})\sim$10-15, huge systematic bias corrected by mode projection at cost of $\sigma(f_{NL})\sim$20-25.

- **LSST forecast:** expected statistical $\sigma(f_{NL}) < 1$, systematic bias for a contamination model $f_{NL}\sim30$, correcting bias leads to conservative forecast $\sigma(f_{NL})\sim 5$.

- Actual survey systematics can be mapped / mitigated more optimally *(Industrial scale version implemented in DES pipeline)*.

- End-to-end simulations of survey transfer function should include systematics *(Implemented in DES BCC-UFig image simulations)*.

http://www.earlyuniverse.org/release-of-the-sdss-systematics-templates/

Poster advert!

Controlled Experiments in Galaxy Formation

Nina Roth

Genetically modified halos: Experiments in galaxy formation

Nina Roth [n.roth@ucl.ac.uk]

Introduction

Abstract We propose a method to generate *modified initial conditions (ICs)* in high-resolution simulations of galaxy formation in a cosmological context. Building on the Hoffman-Ribak algorithm, we start from a reference simulation with fully random initial conditions, then *make controlled changes to specific properties of a single halo* (such as its mass and merger history). The algorithm makes minimal changes to other properties of the halo and its environment, allowing us to isolate the impact of a given modification.

Constrained realisations The initial density contrast field of a cosmological simulation, $\vec{\delta}$, is a realisation of a Gaussian random field with covariance $\mathsf{C}_0 = \langle(\vec{\delta}-\vec{\mu}_0)^\dagger(\vec{\delta}-\vec{\mu}_0)\rangle$ and mean $\langle\vec{\delta}\rangle = \vec{\mu}_0$. Imposing a constraint – expressed by a constraint vector $\vec{\delta}\cdot\vec{\alpha} = d$ with $d \in \mathbb{C}$ – is equivalent to multiplying the original probability distribution by a penalty function, leading to a new probability density with different mean and covariance. Several such constraints can be applied in succession, and the constrained property can be anything *linearly related to the density contrast*, including angular momentum. **Refer to Roth, Pontzen & Peiris (2015) for full details and derivations.**

Modifying halos Our approach differs from previous studies because we directly modify the halo. For this we select the halo particles identified by a Friends-of-friends (FoF) algorithm at $z = 0$, and trace them back into the initial conditions. We then modify this *proto-halo* by constraining the overdensity of its particles, and run the simulation again until $z = 0$. This new simulation can then be directly compared to the result of the *reference run*.

Results: Density constraints

We demonstrate our technique by constraining a halo's *collapse time* (given by the slope of its mass accretion history, see Wechsler et al. 2002). For this, we keep the density averaged over all halo particles the same, but enhance or decrease the density of the 10% of particles in the innermost region in the proto-halo (top figure). While the total mass at $z = 0$ remains unchanged, the halo assembly and its density profile differ significantly (bottom figure).

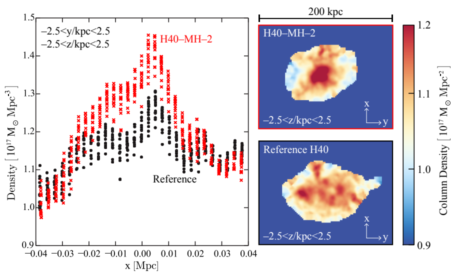

Left panel: The density of the reference ICs (black circles) and modified H40-MH-2 ICs (red crosses) for a collapse constraint where the density of the 10% innermost particles is increased by a factor of 2. The slice is 5 kpc wide in the y- and z-coordinates, to give an impression of the 3D structure. Each symbol corresponds to a single particle/initial grid point. The constrained density field maintains the complicated (sub-)structure that was present in the reference run. **Right panels**: The same two ICs as a 2D projection in the $x-y$-plane. Only those particles that form each halo at $z = 0$ are shown here; it is these particles that are used for generating the constraint in our algorithm. The higher central density is clearly visible in the constrained case (upper panel).

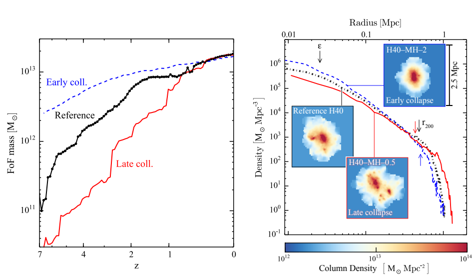

Left panel: Mass accretion history for an *early* (red solid) and *late collapse* (blue dashed) constraint, expressed by the FoF mass (all particles assigned by the halo finder). The black solid line with points shows the same halo in the reference run; each point is one snapshot, illustrating the time resolution of our simulations. **Right panel:** Density profile of the reference halo (black dot-dashed) and the *early* (blue dashed) and *late* (red solid) constrained runs at $z = 0$. The leftmost arrow indicates the softening length of the simulation, and the other arrows indicate the virial radius of each halo. *Inset panels:* density projection ($x-y$-plane) of the resulting halos at $z = 0$. All panels show a region 2.5 Mpc across, include only the FoF group particles, and use the same colour scale for the column density.

Results: Halo concentration

The change in density profile from the collapse constraint can be expressed by the *concentration parameter* $c = \frac{r_{200}}{r_s}$, where r_{200} is the virial radius and r_s is the scale radius in the NFW density profile. The *collapse time* is defined by fitting an exponential to the mass accretion history. These two quantities have been shown to correlate, albeit with significant scatter (e. g. Wechsler et al. 2002). We show the results of constraining three different halos (identified by their halo finder ID), and where they fall on this correlation.

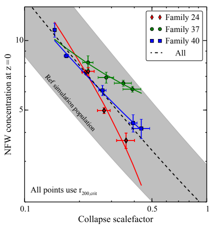

Above: Concentration-collapse time relation of three constrained halo families (halos 24, 37 and 40). The solid coloured lines show fits to each halo family individually and the black dashed line shows a fit to all halos together. The grey band show the average scatter of this relation obtained from a large sample of halos from the reference run, consistent with other studies (e. g. Wechsler et al. 2002). Understanding the origin of the different slopes for each halo family can provide physical insight into this empirical scaling relation.

Results: Constraint probability

A naive choice of constraints can easily result in extreme configurations which are very unlikely to occur within the Hubble volume of the real universe. We can compare the unconstrained and constrained fields with respect to the *unmodified* ΛCDM covariance matrix C_0 by evaluating the change in χ^2, defined as

$$\Delta\chi^2 = \vec{\delta}_n^\dagger \mathsf{C}_0^{-1}\vec{\delta}_n - \vec{\delta}_0^\dagger \mathsf{C}_0^{-1}\vec{\delta}_0, \qquad (1)$$

where $\vec{\delta}_n$ is a field with n constraints. This constrained field has a relative abundance in the universe of $e^{-\Delta\chi^2/2}$ compared to the original, unconstrained field $\vec{\delta}_0$.

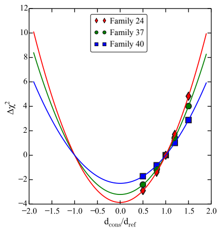

Above: The relationship between $\Delta\chi^2$ and the initial overdensity for three different halo families. Lines show the theoretical prediction from Eq. (1), whereas points give the actual change measured from the IC generator output, confirming that the algorithm is operating as expected.

References

1. Hoffman Y., Ribak E., 1991, ApJ, 380, L5
2. Roth, N., Pontzen, A., Peiris, H. V. 2015, arXiv:1504.07250
3. Wechsler R. H., Bullock J. S., Primack J. R., Kravtsov A. V., Dekel A., 2002, ApJ, 568, 52

Roth, Pontzen & Peiris (2015)


EarlyUniverse@UCL
www.earlyuniverse.org